2021

Experimental and Numerical Study on the Electrical and Thermal Characteristics of High Energy Density Lithium-ion Battery Cell for Application of Battery Electric Vehicle

Ukmin Han
Department of Mechanical Engineering, Korea University, Korea, Republic of (South Korea), castle1992@korea.ac.kr

Hoseong Lee

Experimental and Numerical Study on the Electrical and Thermal Characteristics of High Energy Density Lithium-ion Battery Cell for Application of Battery Electric Vehicle

Ukmin Han[1], Hoseong Lee[1]*

[1]Department of Mechanical Engineering, Korea University,
409 Innovation Hall Bldg., Anam-Dong, Sungbuk-Gu, Seoul, Republic of Korea
Tel: (02) 3290-3355, E-mail: castle1992@korea.ac.kr
*Tel: (02) 3290-3355, E-mail: hslee1@korea.ac.kr

ABSTRACT

In this paper, the electrical and thermal characteristics of the high-energy density of 100 Ah (over 350 Wh/L) pouch-type lithium-ion battery (LIB) cell are analyzed experimentally. To determine the effects of applying current-rate (c-rate) on its behavior, the battery is charged and discharged in different c-rate ranging from 0.5C to 1.2C. The changes in discharged capacity and heat generation rates of battery cells are examined and its mechanism is analyzed deeply in the view of variations on internal resistance. The battery heat generation is considered with two heat sources, joule and entropic heat. A newly developed inverse calculation method is adopted to derive the entropic coefficient in the function of the state of charge. The heat capacity of the battery cell is determined from the convective cooling experiment of battery cell with aluminum block and the combined heat transfer coefficient to calculate the cooling rates of battery cells is also determined appropriately from the Nusselt number correlation. It is confirmed that the numerical model based on the above methods is well suited as a whole from the experiments. In addition, the cell is discharged in different ambient temperature ranging from -15℃ to 45℃ to find out the temperature effects on LIBs. The decrease of capacity and more heat generation of LIB is found under both low and high ambient temperature. As a result, the optimum operating temperature range is redefined as 25℃-35℃ through analyzing the change of electrical and thermal performances of the battery cells.

1. INTRODUCTION

The lithium batteries (LIBs) have been expected to be key solutions to global energy and environmental issues as compared to other secondary batteries. They are used widely in the power industry for energy storage and the automotive industry for the development of sustainable vehicles. However, LIBs are very sensitive to their operating environmental conditions. For instance, their electrochemical performances degrade drastically at a high relative humidity (Chen et al, 2017). A comprehensive review of the thermal effects on LIBs (Ma et al, 2018) indicates the temperature-sensitive characteristics. Pesaran et al. (2013) discovered the optimal operating temperature of the lithium battery cell, showing the cell shows normal performances at the range of 15℃ to 35℃. Nagasubramanian et al. (2000) and Leng et al. (2015) demonstrated that the LIBs experienced a significant performance drop as they are operated deviated from the optimal temperature. Not only the electrical performance drops, but also operating the cell at high ambient temperature could lead to a progressive thermal runaway process, leading to unexpected fire or explosion. Therefore, extensive studies have been conducted from the late 20th century until now to measure the heat generated by LIBs using various experimental methods and modeling approaches. For a decade, various methods have been developed to identify the thermal behaviors of LIBs, and their approaches could be categorized as four groups such as theoretical, experimental, computational, and semi-empirical based models. Theoretical-based models focus to analyze the heat generation of pure electrochemical mechanisms, which are closely related to various related theories like porous electrode theory, concentrated solution theory, electrochemical reaction kinetics theory, and heat transfer model. Typically, P2D or P3D model (Xu et al, 2015) is the representative theoretical-based models. Experimental-based methods directly measure the heat generation rate using calorimetric methods, such as accelerating rate calorimetry and isothermal battery calorimetry. Computational-based models used professional software tools to analyze the thermal behaviors of the battery cell based on well-organized inner theoretical models. Panchal et al. (2018) successfully developed the numerical models that shows a good predictions compared to the experimental values.

Semi-empirical models are the most widely used models because of their simplicity and high accuracy. It concentrates to define the two main heat sources, ohmic and entropic heat, analyzing total heat generation rates in real time. Therefore, at least, two types of experiments are accompanied to calculate both two heat sources. According to the literature review, the semi-empirical model is an intuitive way to identify the thermal characteristics of the battery cell. However, it is extremely limited to find out the models entirely reflecting the actual processes of the battery cells. As some thermal parameters such as specific heat capacity or heat transfer coefficient in convective heat transfer rate, are critically affected by the cell temperature, it should be correctly defined how to use them for developing the robust and high-fidelity of the simulation model. Lastly, most studies have been conducted on LIBs with energy densities ranging from 90 to 300 $Wh \cdot L^{-1}$, which might not be practically used in present and future large-sized battery systems, such as ESS or EVs. Thus, as the demand for LIBs with a much higher energy density has increased considerably, more information and related reports for LIBs with energy density exceeding 300 $Wh \cdot L^{-1}$ are required. In addition, LIBs shows all different thermal behavior according to its type and size, extensive thermal analysis are required either. Therefore, a new transient thermal model is developed for high-energy density lithium battery to overcome the limitations of the abovementioned issues. The thermal parameters, heat capacity and HTC of battery cell, is redefined as a function of cell or ambient temperature. The separate cooling experiment is conducted with the prepared aluminum specimen for comparative analysis with the battery cell. The Nusselt number correlation which reflects the actual operating conditions are adopted to calculate transient convective heat transfer coefficient. Charge and discharge experiments are conducted with different c-rate and ambient temperature. The numerical method of an inverse calculation method is applied to calculate the reversible entropic heat term by deriving the entropic coefficients at each SOC. The developed model is validated with the experimental data, allowing in-depth exploration of thermal characteristics of the battery cell under diverse conditions. The transient cell temperature and heat generation rates are mainly discussed, comprehensively analyzing the related mechanisms.

2. SIMULATION MODEL DEVELOPMENT

2.1 Battery Modeling

The NMC-type pouch cell is used for the current study and its geometrical information is listed in Table 1 with their electrical specifications. The energy density of the battery cell is over 392 $Wh \cdot L^{-1,}$ which is relatively larger than that of the batteries studied earlier. The listed number indicates the representative values reorganized under STP conditions. The operating voltage ranges of the battery cell 2.7 V (for discharge) and 4.2 V (for charge), respectively. It normally discharges under the standard C-rate of 1.0C.

Table 1: Specifications of 100Ah pouch type battery cell

Parameters	Remark	Values
Dimension (mm)	Cell (1)	268×265×13.3
	Tab (2)	80×30×0.28
Internal resistance (mΩ)	Standard	0.55
Weight (g)	-	1,810
Nominal capacity (mAh)	-	100,000
Nominal voltage (V)	-	3.70
Cut-off voltage (V)	charge	4.20
	discharge	2.70
Standard C-rate (C)	-	1.0 (100A)
Max. peak-current (A) (non-continuous at 25ºC)	charge	100
	discharge	300 (10sec)
Life-cycle (at 25ºC)	-	≥ 4000 (80% DOD, 1C/1C)
Recommended operating temperature (ºC)	Charge	10 ~ 35 (1.0C)
	Discharge	-20 ~ 55
	Storage	-20 ~ 25 (>50% R.H.)

2.2 Thermal model development

The transient semi-empirical model is developed based on energy balance of a battery cell (Bernardi et al, 1985) and can be expressed as equation (1):

$$mc_p \frac{dT}{dt} = \dot{Q}_{gen} - \dot{Q}_{conv} - \dot{Q}_{rad} \quad (1)$$

where $\dot{Q}_{gen}$ is the rate of heat generate or consumed during the charge or discharge process of a battery cell. It consists with two main heat sources, joule and entropic heat, as defined as equation (2):

$$\dot{Q}_{gen} = \dot{Q}_{joule} + \dot{Q}_{entropy} = I(V_{oc} - V_{cell}) - IT_{cell}\frac{dV_{oc}}{dT_{cell}} \quad (2)$$

The $\dot{Q}_{joule}$ is the irreversible joule heat generated by the applied current I (positive for charge and negative for discharge) and overpotential, which is the difference between the operating voltage and OCV of the battery cell. This overpotential is caused by the internal resistance of the battery cell and is generally affected by the cell's SOC, operating c-rate, and given environmental conditions. The $\dot{Q}_{entropy}$ is the reversible entropic heat caused by the entropy change from an electrochemical reaction. This reversible term can be both endothermic and exothermic depending on the sign of entropic coefficient. For the first cooling sources, the convective heat transfer coefficient is determined following the equation (3). where the h_{conv} is determined from the Nusselt number correlation. The Nusselt number correlation (equation (4)) under conditions of forced convection over a flat plate (Bergman et al, 2011).

$$\dot{Q}_{conv} = h_{conv} \cdot A \cdot (T_{cell} - T_{amb}) \quad (3)$$

$$Nu = \frac{h_{conv}L_c}{k} = 0.664Re^{1/2}Pr^{1/3} \quad (4)$$

The radiative heat transfer rate is estimated with equation (5) and radiative heat transfer coefficient is calculated using equation (6):

$$\dot{Q}_{rad} = h_{rad} \cdot A \cdot (T_{cell} - T_{surr}) \quad (5)$$

$$h_{rad} = \varepsilon\sigma \cdot (T_{cell} + T_{surr}) \cdot (T_{cell}^2 + T_{surr}^2) \quad (6)$$

The emissivity, ε, is assumed to be 1.0 referred to the earlier studies (Hatchard et al, 2000). The surrounding wall temperature, T_{surr}, is same as the ambient air temperature. To sum up, the transient model is developed by integrating all above equations and used to analyze the transient behaviors of the battery in terms of thermal and electrical characteristics.

2.3 Determination of effective heat capacity of battery cell

The separate cooling experiment is conducted prior to operating the battery cell with prepared aluminum (Al) specimen having the same size of the battery cell. Using the environmental chamber both the Al specimen and the battery cell are heated to 60℃ and directly cooled down to 1℃. As the specific heat capacity of the Al is well known as approximately 880 to 920 $J \cdot kg^{-1} \cdot K^{-1}$ at 0–60℃, the effective heat capacity of the battery cell can be deduced from measuring the cooling rates in real-time using Eq. (7):

$$q''_{cool} = h\Delta T \quad (7)$$

The heat flux q''_{cool} from cooling process is identically applied the Al specimen and the battery cell. The cooling coefficient h can be assumed to be same for both the Al specimen and the battery cell as their geometry is equal.

To summarize, the cooling coefficient can be finally organized as Eq. (8):

$$h = \left[\frac{mc_p}{dt}\frac{(T - T_{air})}{(T_i - T)}\right]_{Al\ specimen} = \left[\frac{mc_p}{dt}\frac{(T - T_{air})}{(T_i - T)}\right]_{cell} \quad (8)$$

Figure 1 illustrates the temperature measurement points of the aluminum specimen, battery cell, and ambient air, respectively.

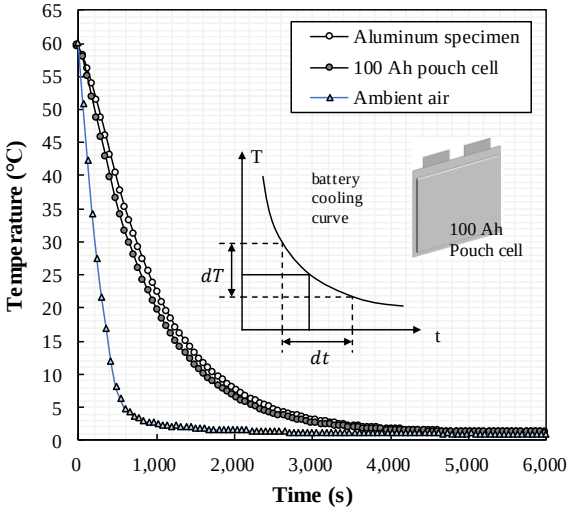

Figure 1: 100 Ah pouch type battery cell

From the cooling experiment, the specific heat capacity is derived as the function of cell temperature. The final form of specific heat capacity of the battery cell is depicted as Eq. (9):

$$c_{p,cell} = -7.2T_{cell}(℃) + 1283.9 \quad (9)$$

2.4 Reversible entropic heat

Entropic heat is one of the most important term in determining the overall heat generation of the battery cell. It is conventional to estimate the entropic coefficients in every SOC, which is typically calculated form the relation between OCV and temperature of the battery cell by progressively discharging the battery cell. However, this conventional method has a great problem of maintaining a perfect electrical-thermal equilibrium state at each measurement. Therefore, the current study applies the numerical iteration of an inverse calculation method to derive entropic coefficients of the battery cell at 10% intervals of SOC. The iterative process is followed by the bottom steps 1-6

Step 1: Simulate the developed thermal model, extracting the cell temperature profiles and calculating the temperature deviations from the experimental values at each time steps. In the first calculation, the entropic heat term is omitted

Step 2: Calculate the required heat at each time step with known materials properties of the battery cell to match the temperature profiles from simulation to those of experiment as shown in Eq. (10):

$$m \cdot \begin{bmatrix} c_{p,t_1} & 0 & 0 & 0 \\ 0 & c_{p,t_2} & 0 & 0 \\ 0 & 0 & \ddots & 0 \\ 0 & 0 & 0 & c_{p,t_f} \end{bmatrix} \begin{bmatrix} dT_{t_1} \\ dT_{t_2} \\ \vdots \\ dT_{t_f} \end{bmatrix} = \begin{bmatrix} \dot{Q}_{t_1} \\ \dot{Q}_{t_2} \\ \vdots \\ \dot{Q}_{t_f} \end{bmatrix} \quad (10)$$

Step 3: Derive the entropic coefficients from the 2nd term following Eq. (11):

$$\begin{bmatrix} \dot{Q}_{t_1} & 0 & 0 & 0 \\ 0 & \dot{Q}_{t_2} & 0 & 0 \\ 0 & 0 & \ddots & 0 \\ 0 & 0 & 0 & \dot{Q}_{t_f} \end{bmatrix} \begin{bmatrix} \left(IT_{cell_{t_1}}\right)^{-1} \\ \left(IT_{cell_{t_2}}\right)^{-1} \\ \vdots \\ \left(IT_{cell_{t_f}}\right)^{-1} \end{bmatrix} = \begin{bmatrix} (dV_{oc}/dT_{cell})_{t_1} \\ (dV_{oc}/dT_{cell})_{t_2} \\ \vdots \\ (dV_{oc}/dT_{cell})_{t_f} \end{bmatrix} \tag{11}$$

Step 4: Linearly interpolate the calculated entropic coefficient at each 10% interval of the SOC.
Step 4: Estimate the entropic heat from the estimated entropic coefficients at each 10% SOC, recalculating the temperature profiles of the battery cell from developed thermal model.
Step 6: repeat the step 1 until satisfying the predefined convergence criteria.
By the above inverse calculation method, it is possible to effectively derive the exact entropic coefficients of the battery cell without the separate experiment. A number of iterations are conducted until the overall errors are within in predefined error range. As a result, new entropic coefficients are estimated, as shown in Figure 2. The other entropic coefficients from previous paper (Forgez et al. (2010), Abdul-Quadir et al. (2014), Liu et al. (2014)) are presented together for comparison to demonstrate a similar trend of the newly obtained entropic coefficients.

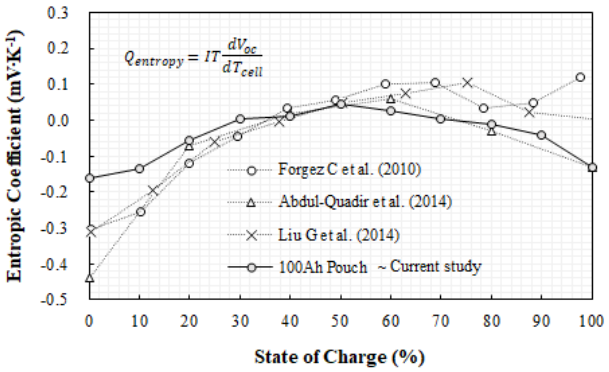

Figure 2: Derivation of entropic coefficients

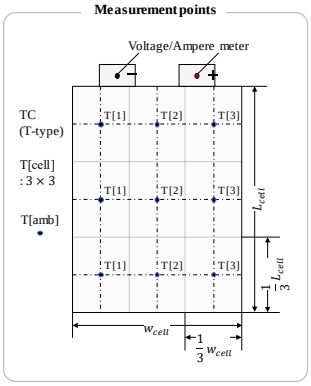

Figure 3: Main measurement points

3. Experiment

The experimental setup comprises three main equipment: a battery cycler, environmental chamber, and a data acquisition system. The battery cell is fixed in the battery jig and connected to the electrical cables.

Table 2: Test matrix for the experimental study

Test	Variable	
Mode	C-rate (C)	Amb. temperature (°C)
Charge (CC-CV) Discharge (CC)	0.5, 0.7, 1.0, 1.2	25
Discharge (CC)	1.0	-15, -5, 5, 15, 25 25, 35, 45

Ten thermocouples sensor are used, nine of which are attached to the top of the battery cell and the last on inside the chamber, to measure the average surface temperature of the battery cell. The main measurement points for the applying current, voltage, and temperature are shown in Figure 3. An anemometer is installed inside the environmental chamber to determine the environmental air-flow conditions. The test matrix for the experimental study are specifically listed in Table 2.

4. Results and discussion

4.1 Model validation

The temperature profiles from the discharging of the battery cell under various c-rate are presented in Figure 4. When comparing the profiles from the simulation and experiment, the maximum errors for each case are within 2.0%. Conclusively, all simulation results show a good agreement with the experimental results. From the validated thermal model, the transient heat generation of battery cell are estimated and the temperature profiles according to the heat generation are illustrated in Figure 5. It depicts the increase in cell temperature through the varying heat generation of the battery cell, showing explicit trends of high heat generation rates occurring in the early and final stages of the operation. This is because of the increased internal resistance of the battery cell. The average uncertainties () are shown together to show the reliability of the output parameters.

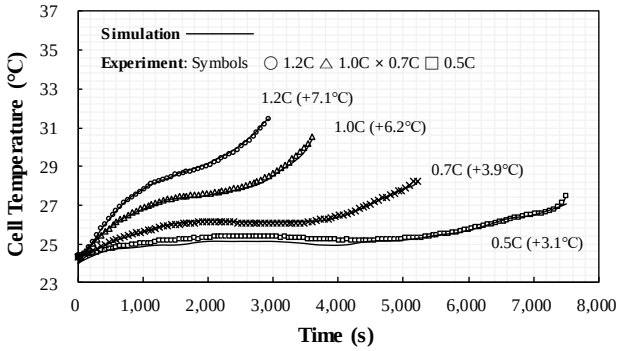

Figure 4: Simulation model validation

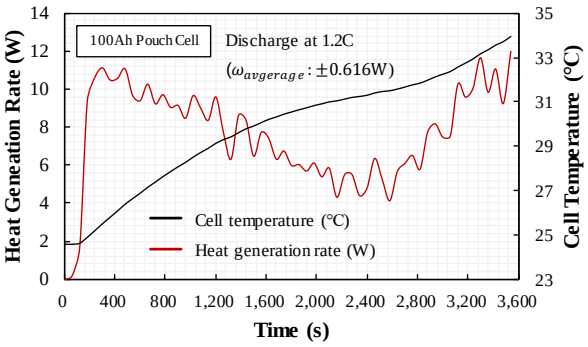

Figure 5: Variations in cell temperature in discharge

4.2 Influences of current-rate

Table 3 show the summary of thermal analysis with the proportion of joule heat. The higher the C-rate, the higher is the ratio of joule heat. This is entirely because of the increment in the current flowing inside the battery cell while the entropic coefficients remain constant.

Table 3: Summary of thermal analysis with different current-rate

Test mode	Current-rate (C)	Heat generation rate (W)	Joule heat ratio (%)
Charge	0.5	2.515	64.1
	0.7	4.072	72.8
	1.0	7.024	79.3
	1.2	9.385	81.6
Discharge	0.5	2.204	78.6
	0.7	3.926	84.8
	1.0	7.356	89.6
	1.2	9.498	97.2

For the charge, the overall proportion of joule heat is varied from 64.1 to 81.6%, and the change in the proportion of joule heat is not as much as that for the discharge. From 0.5C to 1.2C, the joule heat ratio increases simultaneously by 375.2% and 25.5% for the charge and 432.7% and 23.6% for the discharge curves. The ratio of joule heat is also smaller in the charging cycle because the total amount of electric current is reduced in the CV mode.

4.3 Influences of ambient temperature

As the batteries are used in various applications including EVs and ESS, many studies have been conducted to maintain the battery cell at the desired temperature. It is widely known that batteries function satisfactorily at room temperature (25℃) and the deviation from the room temperature can adversely affect the overall chemical reactions of a battery cell. For instance, the liquid-state electrolyte inside a LIB is substantially impacted as the viscosity of the electrolyte varies with temperature, fundamentally affecting the transport rate of lithium ions during the operation. This could lead to other reductions in ionic conductivity and increments of the activation energy and charge-transfer resistance. At high temperatures, the electrical-thermal behaviors of the battery cell are known to be very complicated due to continuous thermal abuse. In severe cases, this can lead to a thermal runaway, resulting in serious safety problems.

4.3.1 Effects on thermal performances

The discharge experiments and simulations of the battery cell at the standard c-rate are conducted under four lower ambient temperatures of -15℃, -5℃, 5℃, 15℃, and two higher temperature 35℃, 45℃ than the room temperature (25℃). The heat generation rates of battery cell at the lowest and highest ambient temperature along with standard room temperature are depicted in Figure 6. It is revealed that the heat generation patterns are drastically increased. This is due to the increment of internal resistance of the battery cell, as mentioned above. Interestingly, at higher ambient temperature (45℃), the heat generation rates are similar. Likewise, the cell temperatures under different temperature shows the same tendency, depending on heat generation patterns. The summary of thermal analysis at different ambient temperature are listed in Table 4.

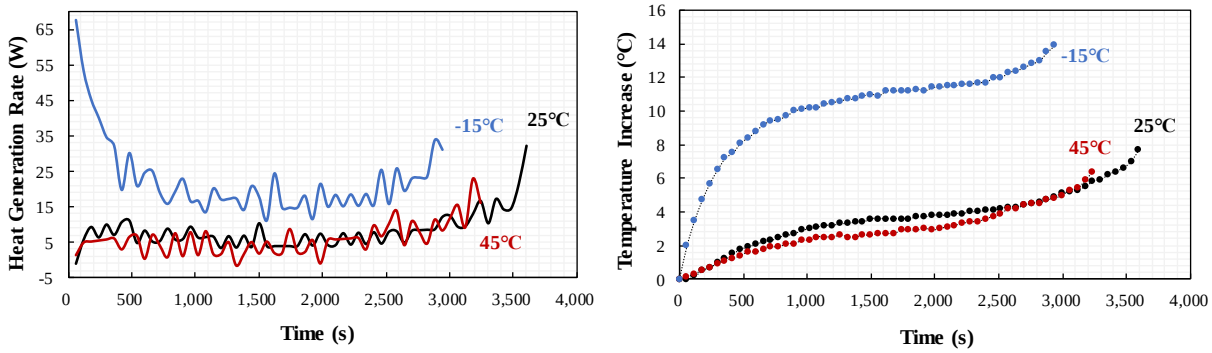

Figure 6: Heat generation rates (left) and cell temperatures (right) under various ambient temperatures

Table 4: Temperature rise and average heat generation of battery cell under different ambient temperature

Ambient temperature (℃)	Cell temperature rise (℃)	Average heat generation rate (W)
-15	13.9	22.59
-5	7.9	12.22
5	7.7	10.78
15	6	7.68
25 (base)	6.2	7.36
35	6.8	6.63
45	6.4	6.04

4.3.2 Effects on electrical performances

Figure 7 directly shows the change rate of electrical performance at low and high ambient temperature, showing that all the capacity and power failure are revealed obviously as deviated from the base temperature of 25°C. When batteries exhibit 100% performance at room temperature, the available capacity of the battery cell at the lowest ambient temperature in ampere-hour is at last decreased by -19.0%. Moreover, the discharge power is reduced by -9.2%. Under high-temperature conditions, the discharge power is also faded. When discharging at 45°C ambient temperature, the cell experiences a decrease of -10.2% in ampere-hour in the available capacity. Similarly, the discharge power is also reduced by -1.3%. The following mechanisms at low temperatures are exactly defined as the

gradually increased internal resistances of the battery cell. The specific factors that cause the internal resistance of the battery include the increase in mass transport resistance of lithium ions inside the electrolyte, increased charge-transfer resistance, and the typical effect of lithium plating. At high temperatures, the reasons for energy loss are the constant thermal treatment of the battery cell, which could lead to a severe loss of capacity. Regarding the electrochemical reaction of the battery cell, thermally induced irreversible crystallographic transformations occur in the cathode material, resulting in irreversible intercalation of lithium ions into the cathode lattice and leading to a loss of the available cathode capacity.

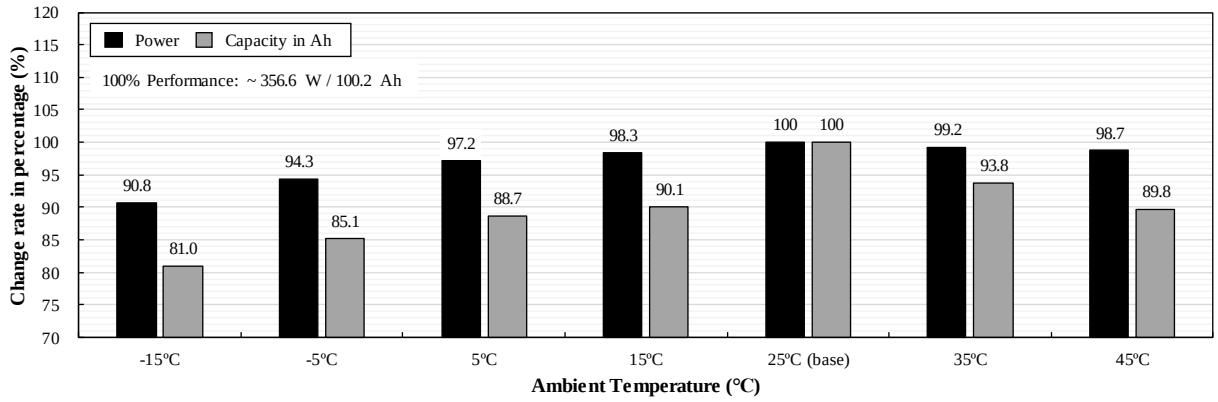

Figure 7: Changes in electrical performances at different ambient temperatures

5. CONCLUSIONS

A transient thermal model is developed to investigate the thermal characteristics of the high-energy-density Li-ion cell. The transient parameters of the effective heat capacity of the battery cell and the heat transfer coefficient are refined to guarantee the high fidelity of the simulation model. A numerical approach of the inverse calculation method is applied to derive the entropic coefficients of the battery cell at specific SOCs. The developed model is validated with the experimental data, predicting exact temperature profiles in real-time. It is used for an in-depth investigation of the battery cell under various operating conditions. The transient thermal behaviors are mainly discussed with different c-rate and ambient temperature. The changes in electrical performances are additionally analyzed to find out the low- and high- temperature effects on the battery cell.

The results from the parametric study are summarized as follows:

- With the increase in c-rate, the joule is become more dominant as the electrical current flow are risen. The heat generation rate is risen to 606% when discharging the cell from 0.5C to 1.2C
- Under lower ambient temperature, gradual performance degradation of the battery capacity and power is found below the room temperature of 25°C. At -15°C, the discharge capacities (Ah) of battery cell decrease by maximum -19.0% compared to those at room temperature. Due to the increase in internal resistance, the cell generates more heat at a low temperature despite less total operation time. (text)
- At higher ambient temperatures, the heat generation rates remain similar compared to the room temperature. However, the available capacity is dropped with the effect of thermal treatment and thermal aging, which hinder the mass transport of Li-ion to the cathode material.

The study focuses on developing a robust transient model for profoundly analyzing the electrical-thermal behaviors of the battery cells under diverse conditions. From the results, the optimum temperature range could be reconsidered based on the resultant transient heat generation rates and the available capacity of the battery cell. Decisively, it reconsidered as 25–35°C based on the criterion that the battery presents 90% of the performance shown in normal operation.

NOMENCLATURE

A	area	(m^2)
Al	aluminum	(-)
CC	constant current	(-)
CV	constant voltage	(-)

c-rate	current-rate	(C)
c_p	specific heat	($kJ \cdot kg^{-1} \cdot K^{-1}$)
EV	electric vehicle	(-)
ESS	energy storage system	(-)
h	cooling coefficient	($W \cdot m^{-2} \cdot K^{-1}$)
I	current	(A)
k	thermal conductivity	($W \cdot m^{-2} \cdot K^{-1}$)
L_c	characteristic length	(m)
m	mass	(kg)
NMC	nickel manganese cobalt	(-)
LIBs	lithium ion batteries	(-)
Nu	Nusselt number	(-)
OCV	open-circuit voltage	(-)
Pr	Prandtl number	(-)
$\dot{Q}$	heat generated or transferred	(W)
Re	Reynolds number	(-)
SOC	state of charge	(-)
t	time	(s)
T	temperature	(°C)
ε	emissivity	(m^2)
σ	Stefan-Boltzmann constant	(m^2)
Δt	timestep	(s)

Subscript

amb	ambient
cell	battery cell
conv	convective
gen	(heat) generation
i	initial
oc	open-circuit
rad	radiative
surr	heat generation
cool	cooling

REFERENCES

Chen, Z., Wang, J., Huang, J., Fu, T., Sun, G., Lai, S., ... & Zhao, J. (2017). The high-temperature and high-humidity storage behaviors and electrochemical degradation mechanism of LiNi0. 6Co0. 2Mn0. 2O2 cathode material for lithium ion batteries. *Journal of Power Sources*, *363*, 168-176.

Ma, S., Jiang, M., Tao, P., Song, C., Wu, J., Wang, J., ... & Shang, W. (2018). Temperature effect and thermal impact in lithium-ion batteries: A review. *Progress in Natural Science: Materials International*, *28*(6), 653-666.

Pesaran, A., Santhanagopalan, S., & Kim, G. H. (2013). *Addressing the impact of temperature extremes on large format li-ion batteries for vehicle applications (presentation)* (No. NREL/PR-5400-58145). National Renewable Energy Lab.(NREL), Golden, CO (United States).

Nagasubramanian, G. (2001). Electrical characteristics of 18650 Li-ion cells at low temperatures. *Journal of applied electrochemistry*, *31*(1), 99-104.

Leng, F., Tan, C. M., & Pecht, M. (2015). Effect of temperature on the aging rate of Li ion battery operating above room temperature. *Scientific reports*, *5*, 12967.

Xu, M., Zhang, Z., Wang, X., Jia, L., & Yang, L. (2015). A pseudo three-dimensional electrochemical–thermal model of a prismatic LiFePO4 battery during discharge process. *Energy*, *80*, 303-317.

Panchal, S., Mathew, M., Fraser, R., & Fowler, M. (2018). Electrochemical thermal modeling and experimental measurements of 18650 cylindrical lithium-ion battery during discharge cycle for an EV. *Applied Thermal Engineering*, *135*, 123-132.

Bernardi, D., Pawlikowski, E., & Newman, J. (1985). A general energy balance for battery systems. *Journal of the electrochemical society*, *132*(1), 5.

Bergman, T. L., Incropera, F. P., DeWitt, D. P., & Lavine, A. S. (2011). *Fundamentals of heat and mass transfer*. John Wiley & Sons.
Hatchard, T. D., MacNeil, D. D., Stevens, D. A., Christensen, L., & Dahn, J. R. (2000). Importance of Heat Transfer by Radiation in Li-Ion Batteries during hermal Abuse. *Electrochemical and Solid State Letters*, *3*(7), 305.
Forgez, C., Do, D. V., Friedrich, G., Morcrette, M., & Delacourt, C. (2010). Thermal modeling of a cylindrical LiFePO4/graphite lithium-ion battery. *Journal of Power Sources*, *195*(9), 2961-2968.
Liu, C., Neale, Z. G., & Cao, G. (2016). Understanding electrochemical potentials of cathode materials in rechargeable batteries. *Materials Today*, *19*(2), 109-123.
Abdul-Quadir, Y., Laurila, ., Karppinen, J., Jalkanen, K., Vuorilehto, K., Skogström, L., & Paulasto-Kröckel, M. (2014). Heat generation in high power prismatic Li-ion battery cell with LiMnNiCoO2 cathode material. *International Journal of Energy Research*, *38*(11), 1424-1437.

ACKNOWLEDGEMENT

This research was supported by the Program of the National Research Foundation of Korea (NRF-2019R1C1C1011195)